

# Resonator induced quantum phase transitions in a hybrid Josephson junction

Robert Hussein<sup>1</sup> and Wolfgang Belzig<sup>2</sup>

<sup>1</sup>*Institut für Festkörpertheorie und -optik, Friedrich-Schiller-Universität Jena, D-07743 Jena, Germany*

<sup>2</sup>*Fachbereich Physik, Universität Konstanz, D-78457 Konstanz, Germany*

(Dated: April 2, 2021)

We investigate the Josephson current through a suspended carbon nanotube double quantum dot which, at sufficiently low temperatures, is characterized by the ground state of the electronic subsystem. Depending on parameters like a magnetic field or the inter-dot coupling, the ground state can either be a current-carrying singlet or doublet, or a blocked triplet state. Since the electron-vibration interaction has been demonstrated to be electrostatically tuneable, we study in particular its effect on the current-phase relation. We show that the coupling to the vibration mode can lift the current-suppressing triplet blockade by inducing a quantum phase transition to a ground state of a different total spin. Our key finding is the development of a triple point in the Josephson current parameterized by the resonator coupling and the Josephson phase. The quantum phase transitions around the triple point are directly accessible through the critical current and resilient to moderately finite temperatures. The proposed setup makes the mechanical degree of freedom part of a superconducting hybrid device which is interesting for ultra-sensitive displacement detectors.

## I. INTRODUCTION

The tunnel coupling of quantum dots (QDs) to superconducting leads can open Andreev bound-state channels that may carry a supercurrent<sup>1–4</sup> and, thus, realize Josephson-like junctions<sup>5–10</sup> that might even realize a nontrivial topology.<sup>11–14</sup> The QDs' highly tunable electronic spectra<sup>15–18</sup> makes them in particular interesting for low-dissipation superconducting spintronics<sup>19,20</sup> and quantum computation.<sup>21,22</sup> Ground-state (GS) transitions in such systems have been observed<sup>23–26</sup> and discussed in terms of the spin-orbit interaction<sup>27,28</sup>, topological protection,<sup>29–33</sup> and nonequilibrium transport.<sup>34–37</sup> Remarkably, it was recently demonstrated in carbon nanotube (CNT) quantum dot setups that the electron-phonon interaction can be tailored electrostatically, to even attain attractive electron interaction.<sup>38–40</sup> In combination with superconducting leads, this may enable the design of novel quantum states of matter.<sup>41,42</sup> CNT devices<sup>43–48</sup> are characterized by their small masses and qualify, likewise, as conductors and nanoresonators with high quality factors.<sup>49–51</sup> They have potential applications in lasing<sup>52–55</sup> and serve in the ultra-sensitive detection of masses,<sup>56,57</sup> charge densities,<sup>58</sup> magnetic moments,<sup>59–61</sup> and terahertz frequencies.<sup>62</sup> In order to achieve noise reduction and single-phonon control, ground-state cooling of nanoresonators has been studied experimentally<sup>63,64</sup> and theoretically.<sup>65–67</sup>

In this Letter, we consider a suspended double quantum dot (DQD) resonator that is attached to two s-wave superconductors and exposed to a magnetic field, see Fig. 1(a). The latter controls the Zeeman splitting of the QD levels and results, for a sufficiently strong field, in a triplet ground state suppressing the Josephson current due to its incompatible spin-symmetry with the superconducting condensates.<sup>68</sup> As shown below, we find that the coupling to the resonator can change the total spin of the QD system, and, thus, help to overcome such a triplet blockade. The total spin quantum number serves as an order parameter and we show that it can give rise to a triple point in the quantum phase diagram spanned by the Josephson phase and the resonator coupling. In particular, we illustrate

in Fig. 1(b) that the corresponding quantum phase transitions between ground states of different total spin are directly reflected in the Josephson current. The occurring triple point further manifests in the critical supercurrent, as investigated in

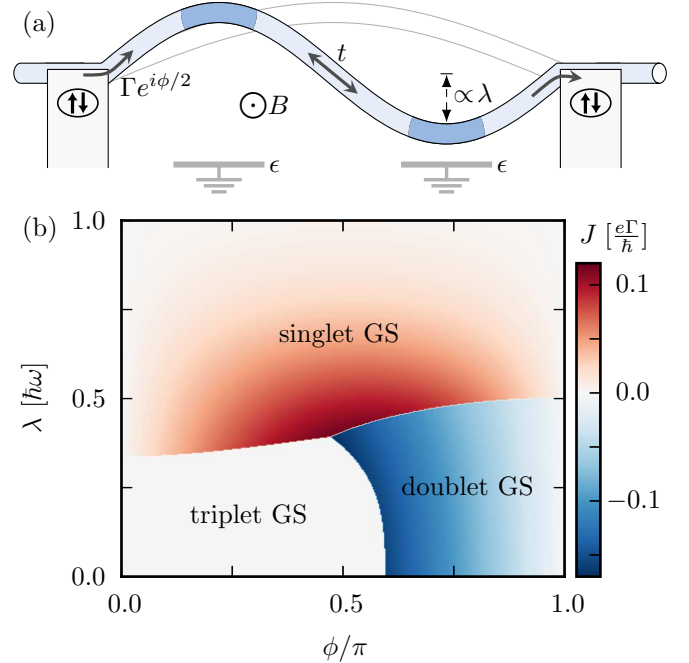


FIG. 1. (a) Carbon nanotube quantum dot subject to a Zeeman field  $B$  and coupled with the rate  $\Gamma$  to two superconducting leads with phase difference  $\phi$ . Depending on the system's ground state, Cooper-pairs may tunnel from one superconductor, via the double quantum dot, to the other establishing, thus, a Josephson current. The coupling  $\lambda$  to the resonator renormalizes the onsite energies  $\epsilon$  of the dots and may change the total spin  $s$  of the system. (b) Josephson current  $J$  in the  $(\phi, \lambda)$ -plane at zero temperature,  $k_B T = 0$ , for the intradot Coulomb interaction  $U_C = t = \Gamma = \hbar\omega$  and  $B = 0.9 \Gamma$ , evaluated at the particle-hole symmetric point,  $\epsilon = -U_C/2$ . It features quantum phase transitions between ground states of different total spin and a common triple point.

$ 0\rangle$	empty state
$ dd\rangle = d_{R\downarrow}^\dagger d_{R\uparrow}^\dagger d_{L\downarrow}^\dagger d_{L\uparrow}^\dagger  0\rangle$	fully occupied
$ S0\rangle = \frac{1}{\sqrt{2}}(d_{R\uparrow}^\dagger d_{L\downarrow}^\dagger - d_{R\downarrow}^\dagger d_{L\uparrow}^\dagger) 0\rangle$	nonlocal singlet
$ S\pm\rangle = \frac{1}{\sqrt{2}}(d_{L\downarrow}^\dagger d_{L\uparrow}^\dagger \pm d_{R\downarrow}^\dagger d_{R\uparrow}^\dagger) 0\rangle$	local singlet
$ T0\rangle = \frac{1}{\sqrt{2}}(d_{R\uparrow}^\dagger d_{L\downarrow}^\dagger + d_{R\downarrow}^\dagger d_{L\uparrow}^\dagger) 0\rangle$	mixed-spin triplet
$ T\sigma\rangle = d_{R\sigma}^\dagger d_{L\sigma}^\dagger  0\rangle$	equal-spin triplet
$ \sigma\pm\rangle = \frac{1}{\sqrt{2}}(d_{L\sigma}^\dagger \pm d_{R\sigma}^\dagger) 0\rangle$	singly occupied
$ t\sigma\pm\rangle = \frac{1}{\sqrt{2}}(d_{L\sigma}^\dagger d_{R\downarrow}^\dagger d_{R\uparrow}^\dagger \pm d_{R\sigma}^\dagger d_{L\downarrow}^\dagger d_{L\uparrow}^\dagger) 0\rangle$	triply occupied

TABLE I. Basis of the system Hamiltonian, subdivided into the singlet (top cell), triplet (middle cell), and doublet sector (bottom cell). Here,  $\sigma = \uparrow, \downarrow$  labels the electron spin.

Fig. 3. To underline the quantum nature<sup>69,70</sup> of the zero temperature phase transitions, we show in Fig. 4 that they smooth out, when thermal fluctuations start to play a role. The central transport features, however, are preserved for experimentally relevant temperatures.

## II. QUANTUM DOT JOSEPHSON JUNCTION

We study the DQD Josephson junction in the limit of a large superconducting gap and consider an Anderson-Holstein type<sup>71-74</sup> system Hamiltonian,

$$H_S = H_{\text{DQD}} + \hbar\omega a^\dagger a + \lambda(a^\dagger + a) \sum_{\sigma} (n_{L\sigma} - n_{R\sigma}), \quad (1)$$

where the occupation imbalance,  $n_{L\sigma} - n_{R\sigma}$ , of the double quantum dot is coupled with the strength  $\lambda$  to a mechanical mode of frequency  $\omega$ . Here,  $a^\dagger$  is the creation operator of the bosonic mode, and  $n_{\alpha\sigma} = d_{\alpha\sigma}^\dagger d_{\alpha\sigma}$  denotes the fermionic occupation operator, where  $d_{\alpha\sigma}^\dagger$  creates an electron on the dot  $\alpha = L, R$  with spin  $\sigma = \uparrow, \downarrow$ . The double quantum dot is modeled by<sup>28,75-77</sup>

$$H_{\text{DQD}} = \sum_{\alpha\sigma} \left( \epsilon + \sigma \frac{B}{2} \right) n_{\alpha\sigma} + \frac{t}{2} \sum_{\sigma} (d_{L\sigma}^\dagger d_{R\sigma} + \text{H.c.}) + \sum_{\alpha} \left[ U_C n_{\alpha\uparrow} n_{\alpha\downarrow} - \frac{\Gamma}{2} (e^{i\phi/2} d_{\alpha\uparrow}^\dagger d_{\alpha\downarrow}^\dagger + \text{H.c.}) \right], \quad (2)$$

where the first term describes the Zeeman splitting of the dot levels with energy  $\epsilon$  due to an applied magnetic field  $B$ . The second term characterizes the interdot tunneling with tunneling amplitude  $t$ . Each dot  $\alpha$  can house up to two electrons of opposite spin which are subject to the intradot Coulomb interaction  $U_C$ . The term  $\propto d_{\alpha\uparrow}^\dagger d_{\alpha\downarrow}^\dagger$  describes the Andreev tunneling of a Cooper-pair with the rate  $\Gamma$  into dot  $\alpha$ , where  $\phi$  is the Josephson phase. We use the convention  $\sigma = \pm$  for the spin up/down and  $\alpha = \pm$  for the left/right dot. The Josephson current<sup>78-81</sup>

$$J = \frac{2e}{\hbar} \partial_{\phi} F(\phi) \quad (3)$$

through the system, is given by the derivative of the free energy  $F = -k_B T \ln Z$  with respect to the phase  $\phi$ . Here,  $Z = \text{tr} e^{-H_S/k_B T}$  denotes the partition function of the canonical ensemble. Since the Josephson current is  $2\pi$ -periodic in  $\phi$  and antisymmetric in  $\phi \rightarrow -\phi$ , we restrict the Josephson phase hereafter to the regime  $0 \leq \phi < \pi$ . The Josephson current is furthermore particle-hole symmetric,  $\epsilon \rightarrow 2\epsilon_0 - \epsilon$ , with  $\epsilon_0 \equiv -U_C/2$ . At zero temperature,  $T = 0$ , Eq. (3) reduces to  $J = (2e/\hbar) \partial_{\phi} E_{\text{GS}}$  with  $E_{\text{GS}}$  being the ground state energy of the system. The diagonalization of the system Hamiltonian  $H_S$  and, therewith, the calculation of the Josephson current is, however, hindered by the coupling to the oscillator. In the following, we will eliminate the oscillator degrees of freedom and derive an effective low-dimensional Hamiltonian for the electronic subsystem.

## III. ELIMINATION OF THE OSCILLATOR

In order to eliminate the electron-phonon coupling term in the system Hamiltonian, Eq. (1), and eventually the oscillator mode, we introduce the polaron transformation<sup>82-85</sup>  $\bar{O} \equiv e^X O e^{-X}$  with  $X = \frac{\lambda}{\hbar\omega} (a^\dagger - a) \sum_{\sigma} (n_{L\sigma} - n_{R\sigma})$ . From the transformations  $\bar{a} = a - (\lambda/\hbar\omega) \sum_{\alpha\sigma} \alpha n_{\alpha\sigma}$  and  $\bar{d}_{\alpha\sigma} = D(\alpha\lambda/\hbar\omega) d_{\alpha\sigma}$  of the bosonic and fermionic operators, respectively, one finds straightforwardly the transformed system Hamiltonian  $\bar{H}_S$ . Here,  $D(z) \equiv \exp(za^\dagger - z^*a)$  denotes the displacement operator generating a coherent state when applied on the phonon vacuum. Finally, we assume a strong coupling to a thermal bath and take the average with respect to the thermal state  $\rho_{\text{osc}} \propto \exp(-\hbar\omega a^\dagger a/k_B T)$  of the oscillator. Then, we obtain the effective Hamiltonian

$$H_{\text{POL}} = \langle \bar{H}_S \rangle_{\text{osc}} - \frac{\lambda^2}{\hbar\omega} \sum_{\alpha\alpha'\sigma\sigma'} \alpha\alpha' n_{\alpha\sigma} n_{\alpha'\sigma'} + \hbar\omega n_B(\omega). \quad (4)$$

The Bose function  $n_B(\omega) = [\exp(\hbar\omega/k_B T) - 1]^{-1}$  in the last term stems from the thermal average  $\langle a^\dagger a \rangle_{\text{osc}}$  of the phonon number operator. It vanishes in the limit of zero temperature. With the aid of the identity  $n_{\alpha\sigma}^2 = n_{\alpha\sigma}$  and the relation  $D(x)D(y) = D(x+y) \exp[i \text{Im}(xy^*)]$ , the effective Hamiltonian becomes

$$H_{\text{POL}} = \sum_{\alpha\sigma} \left( \bar{\epsilon} + \sigma \frac{B}{2} \right) n_{\alpha\sigma} + \frac{t}{2} \sum_{\sigma} (d_{L\sigma}^\dagger d_{R\sigma} + \text{H.c.}) + \sum_{\alpha} \left[ \bar{U}_C n_{\alpha\uparrow} n_{\alpha\downarrow} - \frac{\bar{\Gamma}}{2} (e^{i\phi/2} d_{\alpha\uparrow}^\dagger d_{\alpha\downarrow}^\dagger + \text{H.c.}) \right] + \bar{U} \sum_{\sigma\sigma'} n_{L\sigma} n_{R\sigma'} + \hbar\omega n_B(\omega) \quad (5)$$

with the renormalized onsite energies  $\bar{\epsilon} = \epsilon - \lambda^2/\hbar\omega$ , intradot Coulomb interaction  $\bar{U}_C = U_C - 2\lambda^2/\hbar\omega$ , and tunneling rate  $\bar{\Gamma} = \Gamma \langle D(2\lambda/\hbar\omega) \rangle$ . The thermal average of the displacement operator is given by<sup>86</sup>  $\langle D(z) \rangle = \exp[-(|z|^2/2) \coth(\hbar\omega/2k_B T)]$ . Notice the emergence of the next-to-last term in Eq. (5) describing an effective interdot Coulomb interaction with coupling strength  $\bar{U} = 2\lambda^2/\hbar\omega$ . If not stated

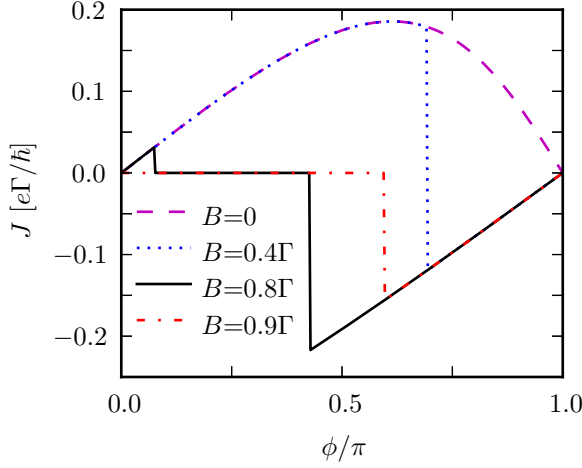


FIG. 2. Josephson current  $J$  as a function of the phase  $\phi$  for different values of the magnetic field  $B$  and vanishing coupling to the oscillator,  $\lambda = 0$ . Parameters are  $\epsilon = -U_C/2$ ,  $t = U_C = \Gamma$ , and  $k_B T = 0$ .

otherwise, we assume the magnetic field to be positive,  $B > 0$ . Its application in the opposite direction,  $B \rightarrow -B$ , would just interchange the spin-up with the spin-down states, but leaves the Josephson current unchanged. The effective Hamiltonian, Eq. (5), is block-diagonal in the singlet, the triplet, and the doublet sector listed in table I, which differ in their total spin quantum number  $s$ . So in order to find the ground-state energy  $E_{GS}$  of the system, one can just diagonalize each sector separately and then determine the lowest eigenvalue. At the particle-hole symmetric point  $\epsilon = \epsilon_0$  one finds that  $E_T = 2\epsilon_0 - |B|$  is the lowest eigenvalue of the triplet sector, and that  $E_D = \frac{1}{2}(E_T - \bar{U} - \sqrt{\bar{\Gamma}^2 + t^2 + 2\bar{\Gamma}t|\sin(\phi/2)|})$  is the lowest eigenvalue of the doublet sector. The lowest eigenvalue of the singlet sector can be estimated by

$$E_S \approx E_S^0 + \frac{\bar{\Gamma}^2(1 + \cos \phi)(E_S^0 - 2\epsilon_0)}{4E_S^0(E_S^0 - \epsilon_0 + \bar{U})} \quad (6)$$

with  $E_S^0 = \epsilon_0 - \bar{U} - \sqrt{(\epsilon_0 + \bar{U})^2 + t^2}$ , see the Appendix. The derivative in  $\phi$  of the ground-state energy  $E_{GS} = \min\{E_S, E_D, E_T\}$  yields, eventually, the estimate

$$J_{\text{est}} \equiv -\frac{e}{\hbar} \begin{cases} \frac{\bar{\Gamma}^2 \sin(\phi)(E_S^0 - 2\epsilon_0)}{2E_S^0(E_S^0 - \epsilon_0 + \bar{U})} & E_S < E_D, E_T \\ \frac{\bar{\Gamma}t \cos(\phi/2) \text{sgn}(\sin(\phi/2))}{2\sqrt{\bar{\Gamma}^2 + t^2 + 2\bar{\Gamma}t|\sin(\phi/2)|}} & E_D < E_S, E_T \\ 0 & E_T < E_S, E_D \end{cases} \quad (7)$$

of the Josephson current at zero temperature.

#### IV. INDUCED QUANTUM PHASE TRANSITIONS AND TRIPLE POINT

First, let us consider the case without the coupling to the resonator,  $\lambda = 0$ , and restrict to zero temperature,  $k_B T = 0$ . In

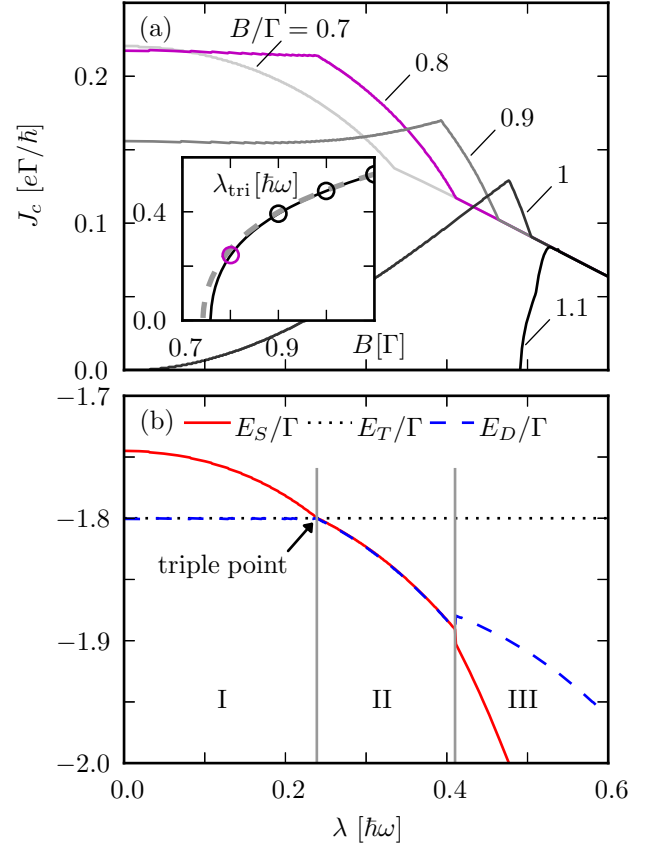


FIG. 3. (a) Critical current  $J_c$  as a function of the oscillator coupling  $\lambda$  for different values of the magnetic field  $B$  and all other parameters as in Fig. 2. The inset shows the coupling strength  $\lambda_{\text{tri}}$  as a function of the magnetic field at which all three ground states coexist. The dashed gray line corresponds to the estimate of the Josephson current given in Eq. (7) and the circles correspond to the magnetic fields in panel (a) for which a triple point emerges. (b) Lowest eigenvalues of the singlet, triplet, and doublet sector corresponding to  $B = 0.8\Gamma$ . The vertical lines indicate phase transitions between distinct ground states.

figure 2, we show the Josephson current  $J$  in dependence of the phase  $\phi$  and choose the parameters such that the QD system is in absence of a magnetic field in a singlet ground state (dashed line). As expected,  $J$  is positive in the interval  $0 < \phi < \pi$ , but shows deviations from the pure sinusoidal behavior due to a finite occupation of the nonlocal singlet state  $|S0\rangle$ . In the limit of vanishing interdot tunneling,  $t \ll \Gamma$ , the nonlocal singlet occupation and, therewith, these deviations cease. At finite magnetic field the lowest eigenenergies of the singlet ( $s = 0$ ), the doublet ( $s = 1/2$ ), and the triplet sector ( $s = 1$ ) are shifted by  $-|sB|$ . Hence, for sufficiently large magnetic field, the system will be in a current suppressing triplet ground state. For intermediate magnetic fields, the Josephson current can feature singlet–doublet (dotted line), triplet–doublet (dot-dashed line), and singlet–triplet (solid line) quantum phase transitions, whereby the doublet ground state reverses the flow of Cooper pairs,  $J < 0$ .

In the following, we study the effect of a finite resonator coupling  $\lambda$  and focus on the configuration exhibiting a triplet–

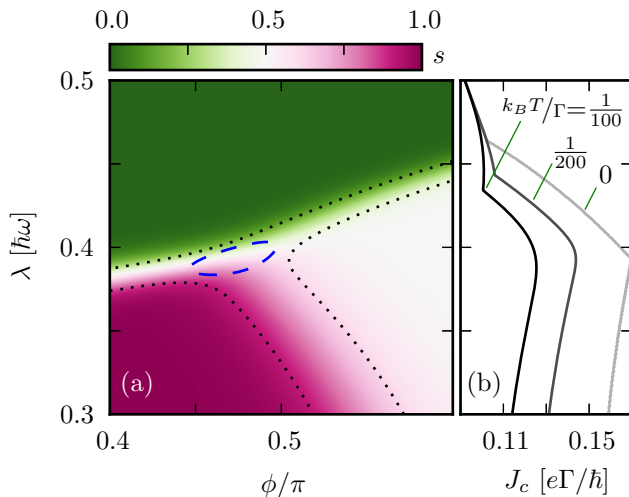


FIG. 4. (a) Total spin quantum number  $s$  as a function of the Josephson phase  $\phi$  and the coupling  $\lambda$  for  $k_B T = \Gamma/200$  and all other parameters as in Fig. 1(b). The dashed and dotted lines indicate the full width at half maximum of the overlaps  $\Pi_{\text{tripel}}$  and  $\Pi_{\text{trans}}$  defined in Sec. V, characterizing the broadening of the triple point and the phase transitions, respectively. (b) Critical current  $J_c$  in dependence of  $\lambda$  for different temperatures  $T$ .

doublet transition (dot-dashed line in Fig. 2). To this end let us revisit Fig. 1(b) showing the phase diagram of the Josephson current as a function of  $\lambda$  and  $\phi$ . One recognizes immediately that it is subdivided into three different regions with sharp transitions at zero temperature. These regions correspond to a triplet (white region), a doublet (blue region), and a singlet ground state (red region) of the QD system. For large enough  $\lambda$  both, the triplet and the doublet ground state, change to a singlet ground state featuring a positive Josephson current  $J$ . Eventually, this current abates for large resonator coupling,  $\lambda \gg \hbar\omega$ . Intriguingly, one also observes the occurrence of a *triple point*, where all three regions have a common point of intersection. It may qualify for high precision measurements of the resonator coupling strength  $\lambda$ .

We will demonstrate hereafter, that such triple point also manifests in the critical current  $J_c = \max_{\phi} J(\phi)$ , which is experimentally easier accessible. Hence, we depict in Fig. 3(a) the critical current in dependence of the resonator coupling  $\lambda$  and for different magnetic fields  $B$ . For a sufficiently large coupling  $\lambda$ , the critical current  $J_c$  becomes independent of the magnetic field, since the DQD assumes then an unmagnetic singlet ground state, as discussed above. For small  $\lambda$ , however, an increasing magnetic field  $B > B_c$  with  $B_c \approx 0.75\Gamma$  reduces the critical current indicating, thus, the presence of a triplet ground state. In particular, the critical current in  $\lambda$  shows up to two characteristic kinks, which for  $B = 0.8\Gamma$  (purple line) are roughly located about  $\lambda \approx 0.24\Gamma$  and  $\lambda \approx 0.41\Gamma$ . For magnetic fields below  $B_c$ , however, the left kink disappears. To better understand the nature of these kinks, we inspect for  $B = 0.8\Gamma$  in panel (b) the corresponding lowest eigenvalues of each sector. One sees, indeed, that the left kink is associated to the triple point and that the right kink corresponds to a transition from a mixed singlet–doublet ground state to a pure

singlet ground state. In the inset of panel (a), we show the coupling strength  $\lambda_{\text{tri}}$  at which, for a given magnetic field  $B$ , a triple point emerges. The required coupling strength  $\lambda_{\text{tri}}$  increases above  $B_c$  with the magnetic field  $B$  (black solid line). Below  $B_c$ , however, no triple point is possible. The dashed gray line indicates the estimated condition for the triple point given in the Appendix. It agrees well with the full calculation, but slightly underestimates the critical Zeeman splitting  $B_c$ .

## V. THERMAL BROADENING OF PHASE TRANSITIONS

While the phase transitions at zero temperature are driven by quantum fluctuations, thermal fluctuations additionally contribute at finite temperature. Their main effect is to smooth out these phase transitions, which is already observable at typical base temperatures of  $T \approx 15\text{--}50$  mK being small against  $\Gamma/k_B$  (ranging from 0.1–1 meV/ $k_B \approx 1\text{--}10$  K).<sup>24,26,87</sup>

For instance, this can be appreciated in figure 4(a) showing the total spin quantum number  $s$  obtained from the thermal average  $\langle S \rangle_{\text{POL}}^2 = \hbar^2 s(s+1)$  over the electronic subsystem.<sup>88</sup> Here,  $S = (\hbar/2) \sum_{\alpha s s'} d_{\alpha s}^\dagger \sigma_{s s'} d_{\alpha s'}$  denotes the spin operator with  $\sigma$  being the vector of Pauli matrices. The dotted black lines in Fig. 4(a) highlight the thermal broadening, indicating the full width at half maximum of  $\Pi_{\text{trans}} \equiv P_S P_T + P_S P_D + P_D P_T$  with  $P_k = \text{tr}_k \rho_{\text{POL}}$  being the cumulative populations of each sector  $k = S, T, D$ . In particular, the triplet–doublet transition is stronger effected by thermal excitations than transitions between magnetic and unmagnetic states. Similarly, the overlap  $\Pi_{\text{tripel}} \equiv P_S P_T P_D$  gives a notion of the thermal broadening of the triple point—its full width at half maximum is indicated by the dashed blue contour line. For increasing temperature,  $T \ll \Gamma/k_B$ , the phase-space volume of  $\Pi_{\text{tripel}}$  grows roughly quadratically. The critical current  $J_c$  (panel b) mainly reduces with growing temperature but preserves its peak about  $\lambda \approx 0.4\hbar\omega$  corresponding to the broadened triple point.

## VI. CONCLUSIONS

The Josephson transport through a carbon nanotube DQD circuit has been investigated. We have shown that the total spin of the DQD system characterizes at zero temperature its ground state and, therewith, the Josephson current through the circuit. For the latter, we have derived an analytical estimate. While singlet and doublet ground states entail a current phase relation of opposite sign, a triplet ground state rather suppresses the Cooper-pair tunneling. We have demonstrated that a finite coupling to the resonator can, indeed, induce quantum phase transitions between these ground states and lift the triplet blockade. A large resonator coupling eventually drives the system into a singlet ground state. In particular, we found that the resonator can induce a triple point in the Josephson current and analyzed under which conditions this happens. Further, we have seen that such triple point also leaves its footprint in the critical current. For experimentally relevant temperatures, thermal fluctuations occur in addition to the quantum

Hamiltonian	basis
$H^{\text{singlet}} = \begin{pmatrix} 2(\epsilon - \epsilon_0) & 2(\epsilon - \epsilon_0) & 0 & 0 & 0 \\ 2(\epsilon - \epsilon_0) & 2(\epsilon - \epsilon_0) & 0 & -i\bar{\Gamma} \sin \frac{\phi}{2} & \bar{\Gamma} \cos \frac{\phi}{2} \\ 0 & 0 & 2\epsilon & 0 & -t \\ 0 & i\bar{\Gamma} \sin \frac{\phi}{2} & 0 & 2(\epsilon - \epsilon_0 - \bar{U}) & 0 \\ 0 & \bar{\Gamma} \cos \frac{\phi}{2} & -t & 0 & 2(\epsilon - \epsilon_0 - \bar{U}) \end{pmatrix}$	$\left\{ \frac{ dd\rangle -  0\rangle}{\sqrt{2}}, \frac{ dd\rangle +  0\rangle}{\sqrt{2}},  S0\rangle,  S-\rangle,  S+\rangle \right\}$
$H^{\text{triplet}} = \text{diag}(2\epsilon + B, 2\epsilon, 2\epsilon - B)$	$\{ T\uparrow\rangle,  T0\rangle,  T\downarrow\rangle\}$
$H^{\text{doublet}} = \begin{pmatrix} \frac{B}{2} \mathbb{1}_2 \otimes \sigma_z + \bar{\epsilon} \mathbb{1}_4 + \frac{t}{2} \sigma_x \otimes \mathbb{1}_2 & \frac{\bar{\Gamma}}{2} \exp[-i\frac{\phi}{2} \sigma_z \otimes \mathbb{1}_2] \\ \frac{\bar{\Gamma}}{2} \exp[i\frac{\phi}{2} \sigma_z \otimes \mathbb{1}_2] & \frac{B}{2} \mathbb{1}_2 \otimes \sigma_z + [\bar{\epsilon} + 2(\epsilon - \epsilon_0)] \mathbb{1}_4 - \frac{t}{2} \sigma_x \otimes \mathbb{1}_2 \end{pmatrix}$	$\{ R\uparrow\rangle,  R\downarrow\rangle,  L\uparrow\rangle,  L\downarrow\rangle,  tR\uparrow\rangle,  tR\downarrow\rangle,  tL\uparrow\rangle,  tL\downarrow\rangle\}$

TABLE II. Decomposition of the effective Hamiltonian  $H_{\text{POL}}|_{k_B T=0} = H^{\text{singlet}} \oplus H^{\text{triplet}} \oplus H^{\text{doublet}}$  at zero temperature into sectors of different total spin. Here,  $\sigma_x, \sigma_y, \sigma_z$  denote the Pauli matrices,  $\mathbb{1}_n$  is the identity matrix in the dimensions  $n \times n$ , and  $\epsilon_0 = -U_C/2$ .

ones. Overall, a finite temperature reduces the supercurrent and washes out the triple point and, hence, the quantum phase transitions. The characteristic transport features, however, still remain.

The proposed hybrid device is an ideal platform for accessing the ultimate limit of a mechanical resonator that is coupled to Cooper pairs traversing a Josephson junction. It not only constitutes a quantum hybrid device based on the fundamental coupling between mechanical and electronic degrees of freedom but also paves the way for ultra-sensitive displacement detectors. A future perspective might be to go beyond the approximation of a thermal resonator state and investigate time-dependent dynamics that is controlled by quantum fluctuations.

### ACKNOWLEDGMENTS

We thank Daniel Reger for contribution to the calculations and Raffael Klees for helpful discussions. R.H. acknowledges financial support from the Carl-Zeiss-Stiftung. W. B. was supported by the Deutsche Forschungsgemeinschaft (DFG, German Research Foundation) Project-ID 32152442 - SFB 767 and Project-ID 425217212 - SFB 1432.

### Appendix A: Josephson current for weakly coupled superconductors

In this section, we provide an estimate of the Josephson current in the limit of weakly coupled superconductors. Since the effective Hamiltonian  $H_{\text{POL}}$  of the main text is block-diagonal in the sectors of different total spin, see table II, each sector can be diagonalized independently. In the following, we calculate the lowest eigenvalue of each sector in order to determine the groundstate energy of the system. Therefrom, we derive the desired estimate of the Josephson current. In the following, we restrict ourselves to the particle-hole symmetric point,  $\epsilon = \epsilon_0$ , and see from table II that

$$E_T = 2\epsilon_0 - |B| \quad (\text{A1})$$

is the lowest eigenvalue of the triplet sector. To find the lowest eigenvalue of the doublet sector, we rewrite the corresponding Hamiltonian as

$$H^{\text{doublet}}|_{\epsilon=\epsilon_0} = \bar{\epsilon} \mathbb{1}_8 + \mathbb{1}_4 \otimes \left[ \frac{B}{2} \sigma_z \right] + \left[ \frac{t}{2} \sigma_z \otimes \sigma_x + \frac{\bar{\Gamma} \cos \frac{\phi}{2}}{2} \sigma_x \otimes \mathbb{1}_2 + \frac{\bar{\Gamma} \sin \frac{\phi}{2}}{2} \sigma_y \otimes \sigma_z \right] \otimes \mathbb{1}_2 \quad (\text{A2})$$

with  $\sigma_k$  Pauli matrices. One immediately recognizes, that the first term just shifts the eigenspectrum by  $\bar{\epsilon}$ . The latter two terms are of the form of a Kronecker sum,  $\mathbb{1}_{\dim Y} \otimes X + Y \otimes \mathbb{1}_{\dim X}$ , with its eigenvalues composed of all pairs of the eigenvalues of  $X$  and  $Y$ <sup>89,90</sup>. While the term corresponding to  $X$  is already diagonal with the eigenvalues  $\pm B/2$ , the term corresponding to  $Y$  features a biquadratic characteristic equation with the four eigenvalues  $\pm \frac{1}{2} \sqrt{\bar{\Gamma}^2 + t^2} \pm 2\bar{\Gamma}t \sin(\phi/2)$ ; both plus-minus signs are independent of each other. By collecting all the mentioned contributions, we find

$$E_D = \bar{\epsilon} - \frac{|B|}{2} - \frac{1}{2} \sqrt{\bar{\Gamma}^2 + t^2 + 2\bar{\Gamma}t |\sin(\phi/2)|} \quad (\text{A3})$$

to be the lowest eigenvalue of the doublet sector. The modulus in the last term takes into account the change of sign of the sine function over a period.

Finally, we estimate the lowest eigenvalue of the singlet sector. Firstly, one observes that  $\frac{1}{\sqrt{2}}(|dd\rangle - |0\rangle)$  becomes a zero-eigenstate at the particle-hole symmetric point. So, the remaining spectrum can be found from the reduced Hamiltonian

$$H_{\bar{\Gamma}} \equiv \begin{pmatrix} 0 & 0 & -i\bar{\Gamma} \sin \frac{\phi}{2} & \bar{\Gamma} \cos \frac{\phi}{2} \\ 0 & 2\epsilon_0 & 0 & -t \\ i\bar{\Gamma} \sin \frac{\phi}{2} & 0 & -2\bar{U} & 0 \\ \bar{\Gamma} \cos \frac{\phi}{2} & -t & 0 & -2\bar{U} \end{pmatrix}. \quad (\text{A4})$$

In absence of the superconductors,  $\bar{\Gamma} = 0$ , its unperturbed eigenvalues read  $E_0^0 = 0$ ,  $E_1^0 = 2\bar{U}$ ,  $E_2 = \epsilon_0 - \bar{U} + \sqrt{(\epsilon_0 + \bar{U})^2 + t^2}$ , and

$$E_S^0 = \epsilon_0 - \bar{U} - \sqrt{(\epsilon_0 + \bar{U})^2 + t^2}, \quad (\text{A5})$$

satisfying  $E_2^0, E_0^0 > E_1^0 > E_S^0$  for  $t, \bar{U} > 0$  and  $\epsilon_0 < 0$ . Hereafter, we will assume that  $t^2 \neq -4\epsilon_0\bar{U}$  for which  $E_2^0$  and  $E_0^0$  become non-degenerate. In the limit of weakly coupled superconductors, one can formally expand the lowest eigenvalue of the singlet sector  $E_S \equiv E_S(\bar{\Gamma})$  to the second order in  $(\bar{\Gamma}/E_S^0)$ ,

$$E_S(\bar{\Gamma}) \approx E_S(0) + \bar{\Gamma}E_S'(0) + \frac{\bar{\Gamma}^2}{2}E_S''(0), \quad (\text{A6})$$

where  $E_S(0) \equiv E_S^0$ . The Taylor coefficients can be related to the characteristic polynomial  $P(\bar{\Gamma}, \lambda) \equiv \det(H_{\bar{\Gamma}} - \lambda \mathbb{1}_4)$  which, in particular, vanishes at the eigenvalue  $\lambda = E_S(\bar{\Gamma})$ . Since also its derivatives have to vanish, one finds from the relation  $0 = \partial_{\bar{\Gamma}}P(\bar{\Gamma}, E_S(\bar{\Gamma}))$  that  $E_S'(0)$  is zero. Similarly, one finds from the second derivative in  $\bar{\Gamma}$  of the characteristic equation,  $0 = \partial_{\bar{\Gamma}}^2P(\bar{\Gamma}, E_S(\bar{\Gamma}))$  and under consideration of  $E_S'(0) = 0$  the relation

$$E_S''(0) = -\frac{P^{(2,0)}(0, E_S^0)}{P^{(0,1)}(0, E_S^0)} = \frac{(1 + \cos \phi)(2\epsilon_0 - E_S^0)}{2E_S^0(E_S^0 - \epsilon_0 + \bar{U})}. \quad (\text{A7})$$

In the last step, we evaluated the derivatives of the characteristic polynomial,

$$P(\bar{\Gamma}, \lambda) = \frac{\bar{\Gamma}^2}{2}(1 + \cos \phi)(2\epsilon_0 - \lambda)(2\bar{U} + \lambda) + \frac{r(\lambda)}{2} [2\lambda(2\bar{U} + \lambda) + \bar{\Gamma}^2(\cos \phi - 1)], \quad (\text{A8})$$

exploiting that the prefactor  $r(\lambda) \equiv (\lambda - 2\epsilon_0)(\lambda + 2\bar{U}) - t^2$  vanishes at  $\lambda = E_S^0$ . Thus, equation (A6) yields the approximation

$$E_S \approx E_S^0 + \frac{\bar{\Gamma}^2(1 + \cos \phi)(E_S^0 - 2\epsilon_0)}{4E_S^0(E_S^0 - \epsilon_0 + \bar{U})} \quad (\text{A9})$$

for the lowest eigenvalue of the singlet sector.

Finally, one obtains from the derivative of the groundstate energy  $E_{GS} = \min\{E_S, E_D, E_T\}$  with respect to the Josephson phase  $\phi$  the estimate of the Josephson current Eq. (7) given in the main text. Moreover, from  $E_T = E_D$  and  $E_T = E_S$  one finds the equations

$$\sin^2 \frac{\phi}{2} = \left[ \frac{\bar{\Gamma}^2 + t^2 - (2\epsilon_0 + \bar{U} - |B|)^2}{2\bar{\Gamma}t} \right]^2, \quad (\text{A10})$$

$$\cos^2 \frac{\phi}{2} = \frac{2E_S^0(\epsilon_0 - \bar{U} - E_S^0)(E_S^0 - 2\epsilon_0 + |B|)}{\bar{\Gamma}^2(E_S^0 - 2\epsilon_0)}, \quad (\text{A11})$$

which, added up,  $\sin^2(\phi/2) + \cos^2(\phi/2) = 1$ , yield a condition for the triple point.

- 
- <sup>1</sup> J-D. Pillet, C. H. L. Quay, P. Morfin, C. Bena, A. Levy Yeyati, and P. Joyez, "Andreev bound states in supercurrent-carrying carbon nanotubes revealed," *Nat. Phys.* **6**, 965 (2010).
  - <sup>2</sup> Eduardo J. H. Lee, Xiaocheng Jiang, Manuel Houzet, Ramon Aguado, Charles M. Lieber, and Silvano De Franceschi, "Spin-resolved Andreev levels and parity crossings in hybrid superconductor-semiconductor nanostructures," *Nat. Nanotechnol.* **9**, 79 (2014).
  - <sup>3</sup> Sun-Yong Hwang, Rosa López, and David Sánchez, "Cross thermoelectric coupling in normal-superconductor quantum dots," *Phys. Rev. B* **91**, 104518 (2015).
  - <sup>4</sup> Sun-Yong Hwang, David Sánchez, and Rosa López, "Nonlinear electric and thermoelectric Andreev transport through a hybrid quantum dot coupled to ferromagnetic and superconducting leads," *Eur. Phys. J. B* **90**, 189 (2017).
  - <sup>5</sup> Mahn-Soo Choi, C. Bruder, and Daniel Loss, "Spin-dependent Josephson current through double quantum dots and measurement of entangled electron states," *Phys. Rev. B* **62**, 13569 (2000).
  - <sup>6</sup> C. Karrasch, A. Oguri, and V. Meden, "Josephson current through a single Anderson impurity coupled to BCS leads," *Phys. Rev. B* **77**, 024517 (2008).
  - <sup>7</sup> Tobias Meng, Serge Florens, and Pascal Simon, "Self-consistent description of Andreev bound states in Josephson quantum dot devices," *Phys. Rev. B* **79**, 224521 (2009).
  - <sup>8</sup> Silvano De Franceschi, Leo Kouwenhoven, Christian Schonberger, and Wolfgang Wernsdorfer, "Hybrid superconductor-quantum dot devices," *Nat. Nanotechnol.* **5**, 703 (2010).
  - <sup>9</sup> A. Martín-Rodero and A. Levy Yeyati, "Josephson and Andreev transport through quantum dots," *Adv. Phys.* **60**, 899 (2011).
  - <sup>10</sup> Nils Wentzell, Serge Florens, Tobias Meng, Volker Meden, and Sabine Andergassen, "Magnetoelectric spectroscopy of Andreev bound states in Josephson quantum dots," *Phys. Rev. B* **94**, 085151 (2016).
  - <sup>11</sup> Roman-Pascal Riwar, Manuel Houzet, Julia S. Meyer, and Yuli V. Nazarov, "Multi-terminal Josephson junctions as topological matter," *Nat. Commun.* **7**, 11167 (2016).
  - <sup>12</sup> R. L. Klees, G. Rastelli, J. C. Cuevas, and W. Belzig, "Microwave Spectroscopy Reveals the Quantum Geometric Tensor of Topological Josephson Matter," *Phys. Rev. Lett.* **124**, 197002 (2020).
  - <sup>13</sup> Julia S. Meyer and Manuel Houzet, "Conductance quantization in topological Josephson trijunctions," arXiv:1911.07705 (2019).
  - <sup>14</sup> H. Weisbrich, R.L. Klees, G. Rastelli, and W. Belzig, "Second Chern Number and Non-Abelian Berry Phase in Topological Superconducting Systems," *PRX Quantum* **2**, 010310 (2021).
  - <sup>15</sup> M. Ciorga, A. S. Sachrajda, P. Hawrylak, C. Gould, P. Zawadzki, S. Jullian, Y. Feng, and Z. Wasilewski, "Addition spectrum of a lateral dot from Coulomb and spin-blockade spectroscopy," *Phys. Rev. B* **61**, R16315 (2000).
  - <sup>16</sup> S. Tarucha, D. G. Austing, T. Fujisawa, and L. P. Kouwenhoven, "Electron Transport in Semiconductor Quantum Dots," in *Optical and Electronic Process of Nano-Matters*, Advances in Optoelectronics (ADOP), Vol. 8 (Springer Netherlands, 2001) p. 57.
  - <sup>17</sup> W. G. van der Wiel, S. De Franceschi, J. M. Elzerman, T. Fujisawa, S. Tarucha, and L. P. Kouwenhoven, "Electron transport through double quantum dots," *Rev. Mod. Phys.* **75**, 1 (2002).
  - <sup>18</sup> M. J. Biercuk, S. Garaj, N. Mason, J. M. Chow, and C. M. Marcus,

- “Gate-Defined Quantum Dots on Carbon Nanotubes,” *Nano Lett.* **5**, 1267 (2005).
- 19 Matthias Eschrig, “Spin-polarized supercurrents for spintronics: a review of current progress,” *Rep. Prog. Phys.* **78**, 104501 (2015).
  - 20 Jacob Linder and Jason W. A. Robinson, “Superconducting spintronics,” *Nat. Phys.* **11**, 307 (2015).
  - 21 T. D. Ladd, F. Jelezko, R. Laflamme, Y. Nakamura, C. Monroe, and J. L. O’Brien, “Quantum computers,” *Nature* **464**, 45 (2010).
  - 22 Frank Arute, Kunal Arya, Ryan Babbush, Dave Bacon, Joseph C. Bardin, Rami Barends, Rupak Biswas, Sergio Boixo, Fernando G. S. L. Brandao, David A. Buell, Brian Burkett, Yu Chen, Zijun Chen, Ben Chiaro, Roberto Collins, William Courtney, Andrew Dunsworth, Edward Farhi, Brooks Foxen, Austin Fowler, Craig Gidney, Marissa Giustina, Rob Graff, Keith Guerin, Steve Habegger, Matthew P. Harrigan, Michael J. Hartmann, Alan Ho, Markus Hoffmann, Trent Huang, Travis S. Humble, Sergei V. Isakov, Evan Jeffrey, Zhang Jiang, Dvir Kafri, Kostyantyn Kechedzhi, Julian Kelly, Paul V. Klimov, Sergey Knysh, Alexander Korotkov, Fedor Kostritsa, David Landhuis, Mike Lindmark, Erik Lucero, Dmitry Lyakh, Salvatore Mandrà, Jarrod R. McClean, Matthew McEwen, Anthony Megrant, Xiao Mi, Kristel Michielsen, Masoud Mohseni, Josh Mutus, Ofer Naaman, Matthew Neeley, Charles Neill, Murphy Yuezhen Niu, Eric Ostby, Andre Petukhov, John C. Platt, Chris Quintana, Eleanor G. Rieffel, Pedram Roushan, Nicholas C. Rubin, Daniel Sank, Kevin J. Satzinger, Vadim Smelyanskiy, Kevin J. Sung, Matthew D. Trevithick, Amit Vainsencher, Benjamin Villalonga, Theodore White, Z. Jamie Yao, Ping Yeh, Adam Zalcman, Hartmut Neven, and John M. Martinis, “Quantum supremacy using a programmable superconducting processor,” *Nature* **574**, 505 (2019).
  - 23 van Dam, A. Jorden, Yuli V. Nazarov, Erik P. A. M. Bakkers, Silvano De Franceschi, and Leo P. Kouwenhoven, “Supercurrent reversal in quantum dots,” *Nature* **442**, 667 (2006).
  - 24 R. Delagrè, R. Weil, A. Kasumov, M. Ferrier, H. Bouchiat, and R. Deblock, “ $0-\pi$  quantum transition in a carbon nanotube Josephson junction: Universal phase dependence and orbital degeneracy,” *Phys. Rev. B* **93**, 195437 (2016).
  - 25 R. Delagrè, R. Weil, A. Kasumov, M. Ferrier, H. Bouchiat, and R. Deblock, “ $0-\pi$  Quantum transition in a carbon nanotube Josephson junction: Universal phase dependence and orbital degeneracy,” *Physica B* **536**, 211 (2018).
  - 26 J. C. Estrada Saldaña, A. Vekris, G. Steffensen, R. Žitko, P. Krogstrup, J. Paaske, K. Grove-Rasmussen, and J. Nygård, “Supercurrent in a Double Quantum Dot,” *Phys. Rev. Lett.* **121**, 257701 (2018).
  - 27 Jong Soo Lim, Rosa López, and Ramón Aguado, “Josephson Current in Carbon Nanotubes with Spin-Orbit Interaction,” *Phys. Rev. Lett.* **107**, 196801 (2011).
  - 28 Stephanie Droste, Sabine Andergassen, and Janine Splettstoesser, “Josephson current through interacting double quantum dots with spin-orbit coupling,” *J. Phys.: Condens. Matter* **24**, 415301 (2012).
  - 29 Pasquale Marra, Roberta Citro, and Alessandro Braggio, “Signatures of topological phase transitions in Josephson current-phase discontinuities,” *Phys. Rev. B* **93**, 220507 (2016).
  - 30 J. Tiira, E. Strambini, M. Amado, S. Roddaro, P. San-Jose, R. Aguado, F. S. Bergeret, D. Ercolani, L. Sorba, and F. Giazotto, “Magnetically-driven colossal supercurrent enhancement in InAs nanowire Josephson junctions,” *Nat. Commun.* **8**, 14984 (2017).
  - 31 Pasquale Marra, Alessandro Braggio, and Roberta Citro, “A zero-dimensional topologically nontrivial state in a superconducting quantum dot,” *Beilstein J. Nanotechnol.* **9**, 1705 (2018).
  - 32 Liliana Arrachea, Alberto Camjayi, Armando A. Aligia, and Leonel Grunero, “Catalog of Andreev spectra and Josephson effects in structures with time-reversal-invariant topological superconductor wires,” *Phys. Rev. B* **99**, 085431 (2019).
  - 33 Gianmichele Blasi, Fabio Taddei, Vittorio Giovannetti, and Alessandro Braggio, “Manipulation of Cooper pair entanglement in hybrid topological Josephson junctions,” *Phys. Rev. B* **99**, 064514 (2019).
  - 34 Marco G. Pala, Michele Governale, and Jürgen König, “Nonequilibrium Josephson and Andreev current through interacting quantum dots,” *New J. Phys.* **9**, 278 (2007).
  - 35 Michele Governale, Marco G. Pala, and Jürgen König, “Real-time diagrammatic approach to transport through interacting quantum dots with normal and superconducting leads,” *Phys. Rev. B* **77**, 134513 (2008).
  - 36 David Futterer, Jacek Swiebodzinski, Michele Governale, and Jürgen König, “Renormalization effects in interacting quantum dots coupled to superconducting leads,” *Phys. Rev. B* **87**, 014509 (2013).
  - 37 Akira Oguri, Yoichi Tanaka, and Johannes Bauer, “Interplay between Kondo and Andreev-Josephson effects in a quantum dot coupled to one normal and two superconducting leads,” *Phys. Rev. B* **87**, 075432 (2013).
  - 38 F. Kuemmeth, S. Ilani, D. C. Ralph, and P. L. McEuen, “Coupling of spin and orbital motion of electrons in carbon nanotubes,” *Nature* **452**, 448 (2008).
  - 39 A. Benyamini, A. Hamo, S. Viola Kusminskiy, F. von Oppen, and S. Ilani, “Real-space tailoring of the electron-phonon coupling in ultraclean nanotube mechanical resonators,” *Nat. Phys.* **10**, 151 (2014).
  - 40 A. Hamo, A. Benyamini, I. Shapir, I. Khivrich, J. Waissman, K. Kaasbjerg, Y. Oreg, F. von Oppen, and S. Ilani, “Electron attraction mediated by Coulomb repulsion,” *Nature* **535**, 395 (2016).
  - 41 M. Margańska, D. R. Schmid, A. Dirnau, P. L. Stiller, Ch. Strunk, M. Grifoni, and A. K. Hüttel, “Shaping Electron Wave Functions in a Carbon Nanotube with a Parallel Magnetic Field,” *Phys. Rev. Lett.* **122**, 086802 (2019).
  - 42 Stefan Blien, Patrick Steger, Niklas Hüttner, Richard Graaf, and Andreas K. Hüttel, “Quantum capacitance mediated carbon nanotube optomechanics,” *Nat. Commun.* **11**, 1636 (2020).
  - 43 J. Schindele, A. Baumgartner, and C. Schönenberger, “Near-Unity Cooper Pair Splitting Efficiency,” *Phys. Rev. Lett.* **109**, 157002 (2012).
  - 44 Minkyung Jung, Jens Schindele, Stefan Nau, Markus Weiss, Andreas Baumgartner, and Christian Schönenberger, “Ultraclean Single, Double, and Triple Carbon Nanotube Quantum Dots with Recessed Re Bottom Gates,” *Nano Lett.* **13**, 4522 (2013).
  - 45 Yutian Wen, N. Ares, F. J. Schupp, T. Pei, G. A. D. Briggs, and E. A. Laird, “A coherent nanomechanical oscillator driven by single-electron tunnelling,” *Nat. Phys.* **16**, 75 (2020).
  - 46 C. Urgell, W. Yang, S. L. De Bonis, C. Samanta, M. J. Esplandiú, Q. Dong, Y. Jin, and A. Bachtold, “Cooling and self-oscillation in a nanotube electromechanical resonator,” *Nat. Phys.* **16**, 32 (2020).
  - 47 Neda Lotfizadeh, Daniel R. McCulley, Mitchell J. Senger, Han Fu, Ethan D. Minot, Brian Skinner, and Vikram V. Deshpande, “Band-Gap-Dependent Electronic Compressibility of Carbon Nanotubes in the Wigner Crystal Regime,” *Phys. Rev. Lett.* **123**, 197701 (2019).
  - 48 D. B. Karki and Mikhail N. Kiselev, “Effects of strong electron interactions and resonant scattering on power output of nano-devices,” *Phys. Rev. B* **100**, 195425 (2019).
  - 49 Andreas K. Hüttel, Gary A. Steele, Benoit Witkamp, Menno Poot, Leo P. Kouwenhoven, and Herre S. J. van der Zant, “Carbon Nanotubes as Ultrahigh Quality Factor Mechanical Resonators,” *Nano Lett.* **9**, 2547 (2009).

- 50 Marc Ganzhorn and Wolfgang Wernsdorfer, “Dynamics and Dissipation Induced by Single-Electron Tunneling in Carbon Nanotube Nanoelectromechanical Systems,” *Phys. Rev. Lett.* **108**, 175502 (2012).
- 51 J. Moser, A. Eichler, J. Güttinger, M. I. Dykman, and A. Bachtold, “Nanotube mechanical resonators with quality factors of up to 5 million,” *Nat. Nanotechnol.* **9**, 1007 (2014).
- 52 Jin-Jin Li and Ka-Di Zhu, “Tunable slow and fast light device based on a carbon nanotube resonator,” *Opt. Express* **20**, 5840 (2012).
- 53 Ke Liu and Volker J. Sorger, “Electrically-driven carbon nanotube-based plasmonic laser on silicon,” *Opt. Mater. Express* **5**, 1910 (2015).
- 54 Mattia Mantovani, Andrew D. Armour, Wolfgang Belzig, and Gianluca Rastelli, “Dynamical multistability in a quantum-dot laser,” *Phys. Rev. B* **99**, 045442 (2019).
- 55 Gianluca Rastelli and Michele Governale, “Single atom laser in normal-superconductor quantum dots,” *Phys. Rev. B* **100**, 085435 (2019).
- 56 A. K. Naik, M. S. Hanay, W. K. Hiebert, X. L. Feng, and M. L. Roukes, “Toward single-molecule nanomechanical mass spectrometry,” *Nat. Nanotechnol.* **4**, 445 (2009).
- 57 J. Chaste, A. Eichler, J. Moser, G. Ceballos, R. Rurali, and A. Bachtold, “A nanomechanical mass sensor with yoctogram resolution,” *Nat. Nanotechnol.* **7**, 301 (2012).
- 58 I. Shapir, A. Hamo, S. Pecker, C. P. Moca, Ö. Legeza, G. Zarand, and S. Ilani, “Imaging the electronic Wigner crystal in one dimension,” *Science* **364**, 870 (2019).
- 59 J.-P. Cleuziou, W. Wernsdorfer, V. Bouchiat, T. Ondarçuhu, and M. Monthieux, “Carbon nanotube superconducting quantum interference device,” *Nat. Nanotechnol.* **1**, 53 (2006).
- 60 M. Urdampilleta, S. Klyatskaya, J.-P. Cleuziou, M. Ruben, and W. Wernsdorfer, “Supramolecular spin valves,” *Nat. Mater.* **10**, 502 (2011).
- 61 Fei Pei, Edward A. Laird, Gary A. Steele, and Leo P. Kouwenhoven, “Valley-spin blockade and spin resonance in carbon nanotubes,” *Nat. Nanotechnol.* **7**, 630 (2012).
- 62 M. Rinzan, G. Jenkins, H. D. Drew, S. Shafranjuk, and P. Barbara, “Carbon Nanotube Quantum Dots As Highly Sensitive Terahertz-Cooled Spectrometers,” *Nano Lett.* **12**, 3097 (2012).
- 63 A. D. O’Connell, M. Hofheinz, M. Ansmann, Radoslaw C. Bialczak, M. Lenander, Erik Lucero, M. Neeley, D. Sank, H. Wang, M. Weides, J. Wenner, John M. Martinis, and A. N. Cleland, “Quantum ground state and single-phonon control of a mechanical resonator,” *Nature* **464**, 697 (2010).
- 64 Jeremy B. Clark, Florent Lecocq, Raymond W. Simmonds, José Aumentado, and John D. Teufel, “Sideband cooling beyond the quantum backaction limit with squeezed light,” *Nature* **541**, 191 (2017).
- 65 P. Stadler, W. Belzig, and G. Rastelli, “Ground-State Cooling of a Carbon Nanomechanical Resonator by Spin-Polarized Current,” *Phys. Rev. Lett.* **113**, 047201 (2014).
- 66 P. Stadler, W. Belzig, and G. Rastelli, “Ground-State Cooling of a Mechanical Oscillator by Interference in Andreev Reflection,” *Phys. Rev. Lett.* **117**, 197202 (2016).
- 67 Mattia Mantovani, Wolfgang Belzig, Gianluca Rastelli, and Robert Hussein, “Single-photon pump by Cooper-pair splitting,” *Phys. Rev. Research* **1**, 033098 (2019).
- 68 James Eldridge, Marco G. Pala, Michele Governale, and Jürgen König, “Superconducting proximity effect in interacting double-dot systems,” *Phys. Rev. B* **82**, 184507 (2010).
- 69 Matthias Vojta, “Quantum phase transitions,” *Rep. Prog. Phys.* **66**, 2069 (2003).
- 70 Vittorio Peano and M. I. Dykman, “Quantum fluctuations in modulated nonlinear oscillators,” *New J. Phys.* **16**, 015011 (2014).
- 71 T. Holstein, “Studies of polaron motion: Part I. The molecular-crystal model,” *Ann. Phys.* **8**, 325 (1959).
- 72 P. W. Anderson, “Localized Magnetic States in Metals,” *Phys. Rev.* **124**, 41 (1961).
- 73 Robert Hussein, A. Metelmann, P. Zedler, and T. Brandes, “Semiclassical dynamics of nanoelectromechanical systems,” *Phys. Rev. B* **82**, 165406 (2010).
- 74 A. Metelmann and T. Brandes, “Adiabaticity in semiclassical nanoelectromechanical systems,” *Phys. Rev. B* **84**, 155455 (2011).
- 75 A. V. Rozhkov and Daniel P. Arovas, “Interacting-impurity Josephson junction: Variational wave functions and slave-boson mean-field theory,” *Phys. Rev. B* **62**, 6687 (2000).
- 76 Robert Hussein, Lina Jaurigue, Michele Governale, and Alessandro Braggio, “Double quantum dot Cooper-pair splitter at finite couplings,” *Phys. Rev. B* **94**, 235134 (2016).
- 77 Robert Hussein, Michele Governale, Sigmund Kohler, Wolfgang Belzig, Francesco Giazotto, and Alessandro Braggio, “Nonlocal thermoelectricity in a Cooper-pair splitter,” *Phys. Rev. B* **99**, 075429 (2019).
- 78 B. D. Josephson, “Supercurrents through barriers,” *Adv. Phys.* **14**, 419 (1965).
- 79 F. Bloch, “Josephson Effect in a Superconducting Ring,” *Phys. Rev. B* **2**, 109 (1970).
- 80 C. W. J. Beenakker, “Three “Universal” Mesoscopic Josephson Effects,” in *Transport Phenomena in Mesoscopic Systems: Proceedings of the 14th Taniguchi Symposium, Shima, Japan, November 10–14, 1991*, edited by Hidetoshi Fukuyama and Tsuneya Ando (Springer, 1992) p. 235.
- 81 A. A. Golubov, M. Yu. Kupriyanov, and E. Il’ichev, “The current-phase relation in Josephson junctions,” *Rev. Mod. Phys.* **76**, 411 (2004).
- 82 I. G. Lang and Yu. A. Firsov, “Kinetic Theory of Semiconductors with Low Mobility,” *JETP* **16**, 1301 (1962).
- 83 T. Brandes and B. Kramer, “Spontaneous Emission of Phonons by Coupled Quantum Dots,” *Phys. Rev. Lett.* **83**, 3021 (1999).
- 84 Gerald D. Mahan, *Many-particle physics*, 3rd ed. (Kluwer Academic, Plenum Publ., 2000).
- 85 Tobias Brandes, “Coherent and collective quantum optical effects in mesoscopic systems,” *Phys. Rep.* **408**, 315 (2005).
- 86 Fernando Domínguez, Sigmund Kohler, and Gloria Platero, “Phonon-mediated decoherence in triple quantum dot interferometers,” *Phys. Rev. B* **83**, 235319 (2011).
- 87 H. Ingerslev Jørgensen, T. Novotný, K. Grove-Rasmussen, K. Flensberg, and P. E. Lindelof, “Critical Current  $0-\pi$  Transition in Designed Josephson Quantum Dot Junctions,” *Nano Lett.* **7**, 2441 (2007).
- 88 The thermal average  $\langle \dots \rangle_{\text{POL}} \equiv \text{tr}(\dots \rho_{\text{POL}})$  over the electronic subsystem is given with respect to the thermal state  $\rho_{\text{POL}} \propto \exp(-H_{\text{POL}}/k_B T)$ .
- 89 Alan J. Laub, *Matrix Analysis for Scientists and Engineers* (SIAM, 2004).
- 90 Åke Björck, *Numerical Methods in Matrix Computations* (Springer, 2015).